

# Radiation Effects on MHD Natural Convection Heat Transfer Flow from Spirally Enhanced Wavy Channel through a Porous Medium

Srinathuni Lavanya

Research Scholar, Mewar University, Rajasthan, India

Damala Chenna Kesavaiah

Research Supervisor, Mewar University, Rajasthan, India

**Abstract** – The objective of this paper is to study the radiation effects on magnetohydrodynamic natural convection heat transfer flow from spirally enhanced wavy channel through a porous medium and a smooth flat wall. A uniform magnetic field is assumed to be applied normal to the insulating walls of the channel. The governing equations of the flow field are solved using regular perturbation technique subject to the appropriate boundary conditions. The solution of the mean part and total solution of the problem have been evaluated analytically for various parameters pertaining to the problem and are presented graphically.

**Key Words:** Free Convection, MHD, Radiation, Chemical reaction, Heat source/ sink

\*\*\*\*\*

## I. INTRODUCTION

The problem of natural convection flows over and through wavy walls has been studied because of its several applications to physical problems. Such physical problems are transpiration cooling of re-entry vehicles and rocket boosters, cross-hatching on ablative surfaces and film vaporization in combustion chambers, geophysics, astrophysics, meteorology, aerodynamics, boundary layer control, as heat exchangers and nuclear reactors.

Radiation effects on the free convection flow are important in the context of space technology and processes involving high temperatures and very little is known about the effects of radiation on free convection flow of radiating fluid confined between two finitely long (compared to the width of the channel) vertical walls, one of which is spirally enhanced (roughed) or wavy. The inclusion of radiation effects in the energy equation however leads to highly nonlinear partial differential equations. Since radiation is quite complicated, its effect on the flow and heat transfer characteristics in the problem described in the literature has not been studied. Umavathi [13] studied mixed convective flow of immiscible viscous fluids confined between a long vertical wavy wall and a parallel flat wall. However, Grief *et al.* [9] have shown that in the optically thin limit, the physical situation can be simplified and, thereby they solved the problem of fully developed radiating laminar convective flow in an infinite vertical heated channel closely following the analysis of Cogley *et al.* [8] who showed that, for an optically thin limit, the fluid does not absorb its own emitted radiation but the fluid does absorb radiation emitted by the boundaries, showed that, for an optically thin nongray gas near equilibrium, the following relation holds:

$$\frac{\partial q_r}{\partial y} = 4(T - T_s)I, \text{ where } I = \int_0^\infty \alpha_\lambda \left( \frac{\partial B_\lambda}{\partial T} \right) w d\lambda$$

$T$  is the temperature,  $q_r$  is the radiative heat flux,  $\alpha_\lambda$  is the absorption coefficient,  $B$  is Planck's function, and subscript  $w$  refers to condition at a wall. Fasogbon [7] studied the

effect of radiation when the integrand is evaluated in the static fluid condition.

Convective flow through a porous medium has application in the field of chemical engineering for filtration and purification processes. In petroleum technology, to study the movement of natural gas oil and water through oil channels/reservoirs and in the field of agriculture engineering to study the underground resources, the channel flows through porous medium have numerous engineering and geophysical applications. Effects of free convection currents on the flow were studied. Ching - Yang Cheng [3] studied combined heat and mass transfer in natural convection flow from a vertical wavy surface in a power-law fluid saturated porous medium with thermal and mass stratification. Rehena Nasrin [15] studied mixed magneto convection in a lid-driven cavity with a sinusoidal wavy wall and a central heat conducting body. Chaudhary and Tara Chand [2] investigated the effect of injection on the three dimensional flow and heat transfer through a vertical parallel plate channel, which is embedded in a porous medium. Takhar and Kumar [12] studied the combined free and forced convection of an incompressible viscous fluid in a porous medium past a hot vertical plate. But they have not studied the flows through wavy channel in a porous medium. Ch Kesavaiah and Venkataramana studied [1] a study of some convective flows with heat transfer effects. Devika *et al.* [5] studied chemical reaction effects on MHD free convection flow in an irregular channel with porous medium. Muthuraj *et al.* [9] studied MHD flow of a couple-stress fluid and a viscous fluid in a vertical wavy porous space with travelling thermal waves and temperature-dependent heat source. Satya Narayana [11] studied the effect of variable permeability and radiation absorption on magnetohydrodynamic (MHD) mixed convective flow in a vertical wavy channel with travelling thermal waves. Ebaid [6] studied the effects of magnetic field and wall slip conditions on the peristaltic transport of a Newtonian fluid in an asymmetric channel.

Previous studies of the flow of heat and mass transfer have focused mainly on a flat wall or a regular channel. It is necessary to study the heat and mass transfer in irregular channels because irregular channels are present in many applications. Fluid flow over wavy boundaries may be observed in several natural phenomena, viz, the generation of wind waves on water, the formation of sedimentary ripples in river channels and dunes in the desert. The analysis of such flows finds application in different areas such as transpiration cooling of re-entry vehicles and rocket booster, cross hatching on ablative surfaces and film vaporization in combustion chambers. In view of these applications Das [15] discussed free convective MHD flow and heat transfer in a viscous incompressible fluid confined between a long vertical wavy wall and a parallel flat wall, Taneja and Jain [16] studied MHD flow with slip effects and temperature dependent heat source in a viscous incompressible fluid confined between a long vertical wavy wall and a parallel flat wall.

In view of the above mention investigation and applications, in this paper we investigate the MHD flow of a viscous fluid between a parallel flat wall and a long wavy wall in the presence of a slip condition taking into account the thermal radiation effects through porous medium. The fluid is sucked through the wall  $y=0$  with the constant suction velocity  $V_0$ . The effects of pertinent parameters entering into the problem have been discussed in detail.

**II.FORMULATION OF THE PROBLEM**

We consider a steady two - dimensional flow of nongray gas near equilibrium in the optically thin limit, between finitely long vertical roughed wall ( $y' = \epsilon^* \cos Kx', |\epsilon^*| < 1, K, \text{ the wave number}$ ) and a parallel flat wall ( $y' = d$ ). The wavy and flat walls are maintained at constant temperatures of  $T_w$  and  $T_1$  respectively. The  $x'$ -axis is along the wall in the upward direction and the  $y'$ -axis is normal to it (Figure 1). The fluid properties are assumed to be constant and the Boussinesq approximation will be used so that the density variation is retained only in the buoyancy term. The viscous dissipative heat is also assumed to be negligible. In the present analysis we shall consider small amplitude wall roughness that is characterized by a certain wavelength  $\lambda = \frac{2\pi}{K}$ . The volumetric heat generation/absorption term in the energy equation is assumed constant.

Assuming that the flow takes place at low concentration we neglect Soret and Doufer effects, the following assumptions are made.

- All the fluid properties except density in the buoyancy force are constant.
- The viscous and magnetic dissipative effects are neglected in the energy equation.

- The volumetric heat source/sink term in the energy equation is constant.
- The magnetic Reynolds number is small so that the induced magnetic field can be neglected.
- The wave length of the wavy wall is large such that  $K_w$  is small.
- The viscous dissipation and work done by pressure are sufficiently small in comparison with both heat flow by conduction and the wall temperatures.
- The electric field is assumed to be zero.

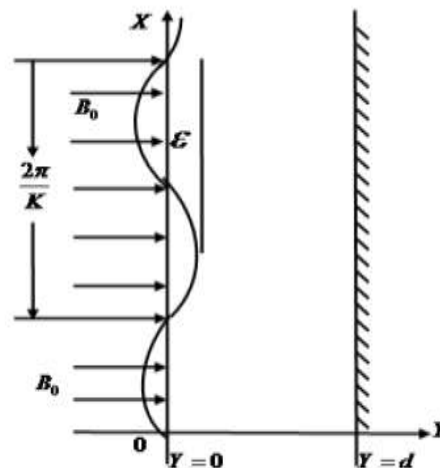


Figure (1): Flow configuration

Under these assumptions the appropriate governing equations of continuity momentum and energy and concentration equations are given by

$$\frac{\partial u'}{\partial X} + \frac{\partial v'}{\partial Y} = 0 \tag{1}$$

$$\rho \left( u' \frac{\partial u'}{\partial X} + v' \frac{\partial u'}{\partial Y} \right) = -\frac{\partial p}{\partial X} + \mu \left( \frac{\partial^2 u'}{\partial X^2} + \frac{\partial^2 u'}{\partial Y^2} \right) - \rho g x - \frac{\mu}{k} u' - \sigma B_0^2 u' \tag{2}$$

$$\rho \left( u' \frac{\partial v'}{\partial X} + v' \frac{\partial v'}{\partial Y} \right) = -\frac{\partial p}{\partial Y} + \mu \left( \frac{\partial^2 v'}{\partial X^2} + \frac{\partial^2 v'}{\partial Y^2} \right) \tag{3}$$

$$\rho C_p \left( u' \frac{\partial T}{\partial X} + v' \frac{\partial T}{\partial Y} \right) = K_T \left( \frac{\partial^2 T}{\partial X^2} + \frac{\partial^2 T}{\partial Y^2} \right) - \frac{\partial q_r}{\partial y} + Q(T - T_s) \tag{4}$$

$$u' \frac{\partial C}{\partial X} + v' \frac{\partial C}{\partial Y} = D \left( \frac{\partial^2 C}{\partial X^2} + \frac{\partial^2 C}{\partial Y^2} \right) - Kr'(C' - C_s) \tag{5}$$

The boundary conditions for velocity, temperature and concentration fields are defined as

$$u' = v' = 0, T = T_w, C' = C_w \text{ at } y' = \varepsilon^* \cos K_w x'$$

$$u' = v' = 0, T = T_1, C' = C_1 \text{ at } y' = d \quad (6)$$

where  $u', v'$  are velocity components in  $x', y'$ -axis respectively,  $B_0$  - transverse magnetic field,  $p$  - pressure,  $T$  - temperature,  $K$  - permeability of the medium,  $k$  is the thermal conductivity,  $\rho$  - density,  $\beta$  - volumetric coefficient of thermal expansion,  $C_p$  specific heat at constant pressure,  $\nu$  - kinematic viscosity, and  $\sigma$  - coefficient of electric conductivity.

Introducing the following non dimensional quantities

$$(x, y) = \frac{1}{d}(X, Y), \quad (u, v) = \frac{d}{\nu}(u', v'), \quad P' = \frac{p'd^2}{\rho\nu^2}$$

$$\theta = \frac{T - T_s}{T_w - T_s}, T_w - T_s \neq 0, C = \frac{C - C_w}{C_w - C_s}, C_w - C_s \neq 0$$

$$a^2 = \frac{d^2}{k'}, \quad \lambda = K_w d, \quad M^2 = \frac{\sigma B_0^2 d^2}{\rho\nu}, \quad R = \frac{4d^2 I}{K_T}$$

$$\alpha = \frac{Qd^2}{K_T(T_w - T_s)}, \quad \text{Pr} = \frac{\mu C_p}{K_T}, \quad \varepsilon = \frac{\varepsilon^*}{d}, \quad \nu = \frac{\mu}{\rho}$$

$$\text{Sc} = \frac{\nu}{d}, \quad m_T = \frac{T_1 - T_s}{T_w - T_s}, \quad m_C = \frac{C_1 - C_s}{C_w - C_s}$$

$$\text{Gr} = \frac{dg_x \beta (T_w - T_s)}{\nu^2}, \quad M^2 = \frac{\sigma B_0^2 d^2}{\nu\rho}$$

In view of the above non-dimensional variables, the basic field equations (1) - (5) can be expressed in the non-dimensional form as

$$\frac{\partial u}{\partial x} + \frac{\partial v}{\partial y} = 0 \quad (7)$$

$$u \frac{\partial u}{\partial x} + v \frac{\partial u}{\partial y} = -\frac{\partial p}{\partial x} + \frac{\partial^2 u}{\partial x^2} + \frac{\partial^2 u}{\partial y^2} - (M^2 + a^2)u \quad (8)$$

$$u \frac{\partial v}{\partial x} + v \frac{\partial v}{\partial y} = -\frac{\partial p}{\partial y} + \frac{\partial^2 v}{\partial x^2} + \frac{\partial^2 v}{\partial y^2} \quad (9)$$

$$\text{Pr} \left( u \frac{\partial \theta}{\partial x} + v \frac{\partial \theta}{\partial y} \right) = \left( \frac{\partial^2 \theta}{\partial x^2} + \frac{\partial^2 \theta}{\partial y^2} \right) - R\theta + \alpha \quad (10)$$

$$\text{Sc} \left( u \frac{\partial C}{\partial x} + v \frac{\partial C}{\partial y} \right) = \left( \frac{\partial^2 C}{\partial x^2} + \frac{\partial^2 C}{\partial y^2} \right) - \text{KrSc} C \quad (11)$$

The corresponding boundary conditions are

$$u = 0, v = 0, \theta = 1, C = 1 \text{ on } y = \varepsilon \cos \lambda x$$

$$u = 0, v = 0, \theta = m_T, C = m_C \text{ on } y = 1 \quad (12)$$

In the static fluid we have

$$\frac{\partial P_s}{\partial x} = \frac{\rho_s g x d^3}{\rho \nu^2} \quad (13)$$

Where

$\rho_s = -\rho \{ 1 + \beta_T (T_w - T_s) \theta + \beta_m (C_w - C_s) C \}$  well known Boussinesq approximation, where subscript  $s$  refers to static conditions,

In view of equation (13), equation (8) becomes

where  $Gr$  is the Grashof number,  $M$  is the Hartmann number,  $\text{Pr}$  is the Prandtl number,  $\nu$  is the kinematic viscosity,  $\varepsilon$  is the non-dimensional amplitude parameter,  $R$  is the radiation parameter,  $\alpha$  is the heat source/sink parameter,  $\phi$  is the dimensionless concentration,  $Kr$  is the chemical reaction parameter,  $\varepsilon$  is the non-dimensional amplitude parameter.

$$u \frac{\partial u}{\partial x} + v \frac{\partial u}{\partial y} = -\frac{\partial}{\partial x}(P - P_s) + \frac{\partial^2 u}{\partial x^2} + \frac{\partial^2 u}{\partial y^2}$$

$$-(M^2 + a^2)u + Gr\theta + GmC \quad (14)$$

### III. SOLUTION OF THE PROBLEM

We assume that the solution consists of a mean part and perturbed part so that the velocity, temperature and concentration distributions are

$$u(x, y) = u_0(y) + u_1(x, y)$$

$$v(x, y) = v_1(x, y)$$

$$P(x, y) = P_0(y) + P_1(x, y) \quad (15)$$

$$\theta(x, y) = \theta_0(y) + \theta_1(x, y)$$

$$C(x, y) = C_0(y) + C_1(x, y)$$

where the perturbed quantities  $u_1, v_1, P_1, \theta_1$  are small compared with the mean or the zeroth order quantities.

Substituting the above Equation (15) into the Equations (7) - (11) and equating the harmonic and non-harmonic terms and neglecting the higher order terms of, we obtain the following set of equations:

The zeroth-order equations

$$\frac{d^2 u_0}{dy^2} - (M^2 + a^2)u_0 + Gr\theta_0 + GmC_0 = K_p \quad (16)$$

$$\frac{d^2 \theta_0}{dy^2} - R\theta_0 = -(\alpha + R) \quad (17)$$

$$\frac{d^2 C_0}{dy^2} - \text{KrSc} C_0 = 0 \quad (18)$$

$$u_0 = 0, \theta_0 = 1, C_0 = 1 \text{ on } y = 0$$

$$u_0 = 0, \theta_0 = m_T, C_0 = m_C \text{ on } y = 1 \quad (19)$$

The first-order equations,

$$\frac{\partial u_1}{\partial x} + \frac{\partial v_1}{\partial y} = 0 \quad (20)$$

$$u_0 \frac{\partial u_1}{\partial x} + v_1 \frac{\partial u_0}{\partial y} = -\frac{\partial P_1}{\partial x} + \frac{\partial^2 u_1}{\partial x^2} + \frac{\partial^2 u_1}{\partial y^2} - (M^2 + a)u_1 + Gr\theta_1 + GmC_1 \quad (21)$$

$$u_0 \frac{\partial v_1}{\partial x} = -\frac{\partial P_1}{\partial y} + \frac{\partial^2 v_1}{\partial x^2} + \frac{\partial^2 v_1}{\partial y^2} \quad (22)$$

$$Pr \left( u_0 \frac{\partial \theta_1}{\partial x} + v_1 \frac{d\theta_0}{dy} \right) = \frac{\partial^2 \theta_1}{\partial x^2} + \frac{\partial^2 \theta_1}{\partial y^2} - R\theta_1 \quad (23)$$

$$Sc \left( u_0 \frac{\partial C_1}{\partial x} + v_1 \frac{dc_0}{dy} \right) = \frac{\partial^2 C_1}{\partial x^2} + \frac{\partial^2 C_1}{\partial y^2} - KrScC_1 \quad (24)$$

$$u_1 = -u_0', v_1 = 0, \theta_1 = \theta_0', C_1 = -C_0' \text{ on } y = 0$$

$$u_1 = 0, v_1 = 0, \theta_1 = 0, C_1 = 0 \text{ on } y = 1 \quad (25)$$

In deriving the first equation in (19) the constant pressure gradient term

Where  $K_p = \frac{\partial}{\partial x}(P_0 - P_s)$  is taken to be zero Vajravelu and Sasatri [19], and a prime denotes differentiation with respect to  $y$ .

To solve the equations (21) - (24) we introduce the following similarity transformations

$$u_1 = -\frac{\partial \psi_1}{\partial y} \text{ and } v_1 = \frac{\partial \psi_1}{\partial x} \quad (26)$$

Eliminating the pressure from (22) and (23) we can express equations (22) - (24) in terms of the stream function  $\psi_1$  in the form

$$u_0 \frac{\partial^3 \psi_1}{\partial x^3} - \frac{\partial^3 \psi_1}{\partial x \partial y^2} - u_0'' \frac{\partial \psi_1}{\partial x} = 2 \frac{\partial^4 \psi_1}{\partial x^2 \partial y^2} + \frac{\partial^4 \psi_1}{\partial x^4} + \frac{\partial^4 \psi_1}{\partial y^4} - (M^2 + a^2) \frac{\partial \psi_1}{\partial y^2} + Gr \frac{\partial \theta_1}{\partial y} - Gm \frac{\partial C_1}{\partial y} \quad (27)$$

$$Pr \left( u_0 \frac{\partial \theta_1}{\partial x} + \frac{\partial \psi_1}{\partial x} \frac{d\theta_0}{dy} \right) = \frac{\partial^2 \theta_1}{\partial x^2} + \frac{\partial^2 \theta_1}{\partial y^2} - R\theta_1 \quad (28)$$

$$Sc \left( u_0 \frac{\partial C_1}{\partial x} + \frac{\partial \psi_1}{\partial x} \frac{dC_0}{dy} \right) = \frac{\partial^2 C_1}{\partial x^2} + \frac{\partial^2 C_1}{\partial y^2} - KrScC_1 \quad (29)$$

We assume  $\psi_1, \theta_1, C_1$ , and in the form

$$\psi_1(x, y) = \varepsilon e^{i\lambda x} \bar{\psi}(\lambda, y)$$

$$\theta_1(x, y) = \varepsilon e^{i\lambda x} \bar{t}(\lambda, y) \quad (30)$$

$$C_1(x, y) = \varepsilon e^{i\lambda x} \bar{\phi}(\lambda, y)$$

(Perturbation series expansion for small wave length  $\lambda$  in which terms of exponential order arise) from which we infer that

$$u_1(x, y) = -\varepsilon e^{i\lambda x} \psi'(\lambda, y)$$

$$v_1(x, y) = \varepsilon i \lambda e^{i\lambda x} \psi(\lambda, y)$$

In view of the above

$$\bar{\psi}^{iv} - i\lambda \left[ u_0 \left( \bar{\psi}'' - \lambda^2 \bar{\psi} \right) \right] - \lambda^2 \left( 2\bar{\psi}'' - \lambda^2 \bar{\psi} \right) =$$

$$Gr\bar{t}' + Gm\bar{\phi}' + (M^2 + a^2)\psi_1'' \quad (31)$$

$$\bar{t}'' - R\bar{t} - \lambda^2 \bar{t} = Pr i \lambda \left[ u_0 \bar{t} + \bar{\psi} \theta_0' \right] \quad (32)$$

$$\bar{\phi}'' - \lambda^2 \bar{\phi} - KrSc\bar{\phi} = Sc i \lambda \left( u_0 \bar{\phi} + \psi C_0' \right) \quad (33)$$

where the primes denote differentiation with respect to  $y$ . The boundary condition (26) can now be written in terms of  $\psi_1$

$$\frac{\partial \psi_1}{\partial y} = u_0', \frac{\partial \psi_1}{\partial x} = 0 \text{ on } y = 0$$

$$\frac{\partial \psi_1}{\partial y} = 0, \frac{\partial \psi_1}{\partial x} = 0 \text{ on } y = 1 \quad (34)$$

For small values of  $\lambda$  (or  $K_w$ ), we can expand  $\bar{\psi}(\lambda, y), \bar{t}(\lambda, y), \bar{\phi}(\lambda, y)$  in terms of  $\lambda$

$$\left. \begin{aligned} \bar{\psi}(\lambda, y) &= \sum_{j=0}^{\infty} \lambda^j \psi_j \\ \bar{t}(\lambda, y) &= \sum_{j=0}^{\infty} \lambda^j t_j \\ \bar{\phi}(\lambda, y) &= \sum_{j=0}^{\infty} \lambda^j \phi_j \end{aligned} \right\}; j = 0, 1, 2, \dots \quad (35)$$

and  $i$  is the complex unit.

Substituting these results into (31) - (33), we obtain the following sets of ordinary differential equations

$$\psi_0^{iv} - (M^2 + a^2)\psi_0'' = Grt_0' + Gm\phi_0' \quad (36)$$

$$t_0'' - Rt_0 = 0 \quad (37)$$

$$\phi_0'' - KrSc\phi_0 = 0 \quad (38)$$

$$\psi_1^{iv} - (M^2 + a^2)\psi_1'' = i(u_0\psi_0'' - u_0''\psi_0) + Grt_1' + Gm\phi_1' \quad (39)$$

$$t_1'' - Rt_1 = iPr(u_0t_0 + \theta_0'\psi_0) \quad (40)$$

$$\phi_1'' - KrSc\phi_1 = iSc(u_0\phi_0 + C_0'\psi_0) \quad (41)$$

$$\psi_2^{iv} - (M^2 + a^2)\psi_2'' = i(u_0\psi_0'' - u_0''\psi_1) + Grt_2' + Gm\phi_2' \quad (42)$$

$$t_2'' - Rt_2 = iPr(u_0t_1 + \theta_0'\psi_1) + t_0 \quad (43)$$

$$\phi_2'' - KrSc\phi_2 = iSc(u_0\phi_1 + \psi_1C_0') + \phi_0 \quad (44)$$

The corresponding boundary conditions are

$$\psi_0' = u_0', \psi_0 = 0, t_0 = -\theta_0', \phi_0 = -C_0' \text{ on } y = 0$$

$$\psi_0' = 0, \psi_0 = 0, t_0 = 0, \phi_0 = 0 \text{ on } y = 1 \quad (45)$$

$$\psi_j' = 0, \psi_j = 0, t_j = 0, \phi_j = 0 \text{ on } y = 0 \text{ for } j \geq 0$$

$$\psi_j' = 0, \psi_j = 0, t_j = 0, \phi_j = 0 \text{ on } y = 1 \quad (46)$$

The solutions of above ordinary differential equations with respect to the boundary conditions (45) and (46) are

$$u(y) = A_1e^{m_1y} + A_2e^{m_2y} + A_3 + A_4e^{m_5y} + A_5e^{m_6y} + A_6$$

$$+ A_7e^{m_{10}y} + A_8e^{m_9y} - \varepsilon[A_{19}y + A_{18}e^{m_9y} + A_{15}e^{m_{10}y}$$

$$+ A_9e^{m_3y} + A_{10}e^{m_4y} + A_{11}e^{m_7y} + A_{12}e^{m_8y}]$$

$$v(y) = -\varepsilon\lambda[A_{21}y^2 + A_{22}e^{m_9y} + A_{23}e^{m_{10}y} + A_{24}e^{m_3y}$$

$$+ A_{25}e^{m_4y} + A_{26}e^{m_7y} + A_{27}e^{m_8y}]$$

$$\theta(y) = L_1 + L_2e^{m_2y} + L_3e^{m_4y} + \varepsilon[L_5e^{m_4y} + L_6e^{m_3y}]$$

$$C(y) = B_1e^{m_6y} + B_2e^{m_5y} + \varepsilon[B_4e^{m_8y} + B_3e^{m_7y}]$$

#### Skin friction

$$\tau = \frac{\partial u}{\partial y} = u_0'(y) - \varepsilon e^{i\lambda x} u_1'(y)$$

$$\tau_{y=0} = m_1A_1 + m_2A_2 + m_5A_4 + m_6A_5$$

$$+ m_{10}A_7 + m_9A_8 - \varepsilon[m_9A_{18} + m_{10}A_{15} + m_9A_9$$

$$+ m_4A_{10} + m_7A_{11} + m_8A_{12}]$$

$$\tau_{y=1} = m_1A_1e^{m_1} + m_2A_2e^{m_2} + m_5A_4e^{m_5} + m_6A_5e^{m_6}$$

$$+ m_{10}A_7e^{m_{10}} + m_9A_8e^{m_9} - \varepsilon[A_{19} + m_9A_{18}e^{m_9}$$

$$+ m_{10}A_{15}e^{m_{10}} + m_3A_9e^{m_3} + m_4A_{10}e^{m_4}$$

$$+ m_7A_{11}e^{m_7} + m_8A_{12}e^{m_8}]$$

The dimensional Nusselt number  $Nu$  is given by

$$Nu = \frac{\partial \theta}{\partial y} = \theta_0'(y) + \varepsilon e^{i\lambda x} \theta_1'(y)$$

$$Nu_{y=0} = m_2L_2 + L_3m_1 + \varepsilon[m_4L_5 + m_3L_6]$$

$$Nu_{y=1} = m_2L_2e^{m_2} + L_3m_1e^{m_1} + \varepsilon[m_4L_5e^{m_4} + m_3L_6e^{m_3}]$$

The dimensional Sherwood number  $Sh$  is given by

$$Sh = \frac{\partial C}{\partial y} = C_0'(y) + \varepsilon e^{i\lambda x} C_1'(y)$$

$$Sh_{y=0} = m_6B_1 + m_5B_2 + \varepsilon[m_8B_4 + m_7B_5]$$

$$Sh_{y=1} = m_6B_1e^{m_6} + m_5B_2e^{m_5} + \varepsilon[m_8B_4e^{m_8} + m_7B_5e^{m_7}]$$

#### Appendix

$$m_1 = m_3 = \sqrt{R}, m_2 = m_4 = -\sqrt{R}$$

$$m_5 = m_7 = \sqrt{KrSc}, m_6 = m_8 = -\sqrt{KrSc}$$

$$m_9 = \sqrt{M^2 + a^2}, m_{10} = -\sqrt{M^2 + a^2}$$

The other constants not shown to brave the space

#### IV. RESULTS AND DISCUSSIONS

The results of the numerical evaluations at various values of  $y$  are displayed in figures (2) – (8) for some dimensionless mean solution (zeroth-order  $u_0, \theta_0$  correspond to fully developed mean flow; applicable to the case of a channel whose walls are both flat), first-order ( $v_1, \theta_1$  arising out of small roughness of a wall of the channel) and the total dimensionless  $u = (u_0 + u_1)$  velocity profiles. We have computed the numerical values of velocity, temperature, skin friction and Nusselt number for cooling of the wall ( $Gr > 0$ ),  $\varepsilon = 0.002$  ( $\varepsilon > 0$  case of dilated channel),  $\lambda = 0.01, 0.02$ . For physical reality, we took wall temperature ratio parameter  $m = -1.0$  when it is postulated that the average of the temperatures of the two walls is equal to that of the static fluid.  $m = 0$  implies that the temperature of the static fluid is equal to that of the flat wall,  $m = 1.0$  means equal wall temperatures while  $m = 2.0$  indicates that wall temperatures are unequal. In the absence of heat generation we have  $\alpha = 0$ , while  $\alpha = 5.0$  corresponds to heat generation and  $\alpha = -5.0$  gives absorption.

Figures (2) – (8) depict the zeroth-order velocity  $u_0$  of the fluid when  $m_c = 1.0$  and  $m_T = 2.0$  with changes in the heat generation parameter ( $\alpha$ ), thermal Grashof number ( $Gm$ ), Grashof number ( $Gr$ ), Chemical reaction parameter ( $Kr$ ), Magnetic parameter ( $M$ ), Schmidt number ( $Sc$ ), and Radiation parameter ( $R$ ).

Qualitatively similar behaviour of the fluid velocity  $u_0$  occurs with an increase in heat generation parameter from figure (2). The aforesaid conclusions hold good in the case of thermal radiation ( $R > 0$ ). However, the only exception is that the velocity in the absence of thermal radiation ( $R = 0$ ) increases across the channel width with in the presence of heat generation. It is clear from figure (3) and (4) that with an increase in the thermal Grashof number ( $Gm$ ) and Grashof number ( $Gr$ ) the magnitude of the zeroth order fluid velocity  $u_0$  increases across the entire channel width. Figure (5) depicts the variation of zeroth order velocity profiles  $u_0$  against for different values of chemical reaction parameter for fixed values of other parameters. It is observed that, increasing the value of chemical reaction results decreases the velocity and concentration in the boundary layer. This is due to fact that destructive chemical reaction reduces the solutal boundary layer thickness and increase the mass transfer. Figure (6) depicts the zeroth order velocity distribution  $u_0$  for different values of magnetic parameter. It observed that the zeroth order velocity decreases with increasing in magnetic parameter. The influence of Schmidt number on the zeroth order velocity profiles are plotted in figure (7). The Schmidt number embodies the ratio of momentum to the mass diffusivity. The Schmidt number therefore quantifies the relative effectiveness of momentum and mass transport by diffusion in the hydrodynamic (velocity) boundary layers. As the Schmidt number increases the velocity increases. Figure (8) shows the zeroth order velocity distribution for different values of radiation parameter. It is observed that the zeroth order velocity distribution increases when the radiation parameter increases.

Figures (9) illustrate the behaviour of the fluid mean temperature  $\theta_0$  with changes in heat absorption when  $m_T = -1.0$ , curves and  $m_T = 2.0$ , curves for non-radiating and radiating respectively. From figure (9) it is evident that for all values of heat absorption, the fluid temperature  $\theta_0$  in the in absence of thermal radiation ( $R = 1.0$ ) while it is parabolic in nature curves increases for its radiating counterpart with  $m_T = -1.0, 2.0$ . Also superimposed on it there are parabolic distributions that are due to the presence of heat generation/absorption for the two cases under consideration. Form figure (10) shows the mean temperature distribution  $\theta_0$  against  $y$  for different values of radiation parameter, it is evident that for all values of, the fluid temperature decreases at  $\alpha = -5.0$  but the temperature is the exact opposite of that observed in the case of  $\alpha = 5.0$ . The effect of radiation is to increase the rate of energy transport to the gas, thereby increasing the temperature of the gas.

Form figures (11) and (12) radically for different values of Chemical reaction parameter and Schmidt number of the concentration profiles are plotted. It is obvious that the effect of increasing values of Chemical reaction parameter and Schmidt number results in a decreasing concentration distribution across the boundary layer.

Figures (13) to (14) show the behaviour of the fluid cross velocity  $v$  perpendicular to the channel length for the effect of buoyancy ( $R > 0$ ) and combined effect of buoyancy and radiation respectively when  $m_C = 1.0$  and  $m_T = 2.0$  each for different values of heat absorption and chemical reaction parameter. It is evident that the  $v$  is affected (enhanced) significantly by the changes in heat absorption and chemical reaction parameter we noticed that as the heat generation parameter is increased  $v$  diminishes sharply and remains negative throughout the channel width. the reverse effect observed in chemical reaction parameter.

Figures (15) and (16) illustrate the behaviour of the total fluid temperature ( $\theta = \theta_0 + \theta_1$ ) when the wall temperature ratio  $m_T = 1.0$  in case under study for different values of heat absorption and radiation parameter. It is obvious that from as the heat absorption is increased the temperature  $\theta$  diminished sharply and positive throughout the width of the channel and the reverse effect observed in radiation parameter.

The variations in the total concentration profiles ( $C = C_0 + C_1$ ) when the wall temperature ratio  $m_C = 1.0$  for different values of Schmidt number and chemical reaction parameter are clearly observed in figures (17) and (18). It is obvious that the concentration decrease with increase in Schmidt number and chemical reaction.

Figures (19) to (23) describe the behaviour of the total fluid velocity  $u = (u_0 + u_1)$  when the wall temperature ratio  $m_C = 1.0$  and  $m_T = 2.0$  respectively under the effect of buoyancy effect ( $R > 0$ ). Increasing values of the radiation parameter, heat absorption parameter, Grashof number, chemical reaction parameter and Magnetic parameter enhance the total velocity considerably. In figures (19) to (22), it is evident that the total velocity is increasing function of increasing  $R, \alpha, Gm, Kr$ . But in the figure (23) the reverse effect observed in magnetic parameter. Figures (24) and (25) show the local skin friction coefficient for different values of  $\alpha$  and at  $y = 0$  and  $y = 1$  keeping all the parameters fixed. From the figure (24) we see that for fixed  $Gr$  at  $y = 0$ ,  $\tau$  increase as  $\alpha$  increases. On the other hand as  $Gr$  increases skin friction coefficient has no effect at  $y = 1$ , against  $\alpha$  in figure (25). Figure (26) and (27) describe the behaviour of rate of heat transfer

$(Nu)$  with changes in the values of  $\alpha$  and  $m_c$  at  $y=0$  and  $y=1$ . It is observed from these figures that the Nusselt number increases due to increases in the heat source parameter  $\alpha$  at  $y=0$  and decreases the heat source parameter  $\alpha$  at  $y=1$  of the walls. Figure (28) and (29) describe the behaviour of Sherwood number ( $Sh$ ) with changes in the values of  $Kr$  and  $m_c$  at  $y=0$  and  $y=1$ . It is observed from these figures that the Sherwood number decreases due to increases in the chemical reaction parameter of the both walls.

### Conclusions

In the present paper, we observed the followings:

- When the Grashof number  $Gr > 0$ , the nature of radiation is to increase the mean velocity and when  $Gr < 0$  then the nature of radiation is to decrease the mean velocity.
- When the Grashof number  $Gr > 0$ , the inclusion of heat source reduces the mean velocity and when  $Gr < 0$  then the inclusion of heat source increases the mean velocity.
- Inclusion of radiation increases and inclusion of heat source reduces the zeroth order temperature.
- The nature of radiation is to decrease the perturbed velocity and secondary velocity for  $Gr > 0$  and to increase these velocities when  $Gr < 0$ .
- The nature of heat source is to increase the perturbed velocity and secondary velocity for  $Gr > 0$  and to decrease these velocities when  $Gr < 0$ .
- Presence of heat source increases the first order temperature near the wall  $y = -1.0$  and after a point where  $y = -0.4$  this temperature decreases with the increase of heat source.
- Existence of radiation reduces the first order temperature near the wall  $y = -1.0$  and after a point where  $y = -0.4$  this temperature increases the increase of radiation.
- When  $Gr > 0$ , the nature of radiation is to reduce the skin friction at the wall  $y = -1$ ,  $y = +1$  and to increase the skin friction at wall  $y = +1$ , but when  $Gr < 0$  the results are opposite to previous statement.
- When  $Gr > 0$ , the inclusion of heat source increases the skin friction at the wall  $y = -1$  and it is decreased at the wall  $y = +1$ , but when  $Gr < 0$  the results are opposite to previous statement.
- Presence of radiation gives a decrement to Nusselt number and increment to recovery factor.

- The Nusselt number changes in the same direction as heat source, but presence of heat source is responsible to reduce the recovery factor.

### References

- [1] D Ch Kesavaiah and S Venkataramana: "A study of some convective flows with heat transfer effects", Ph D Thesis, Sri Venkateswara University, Tirupathi, AP, India, 2011
- [2] Chaudhary and Tara Chand: "Effect of injection through one side of a long vertical channel embedded in porous medium with transpiration cooling", Bull. Cal. Math. Soc., vol.96, No.1, pp.65-70, 2004
- [3] Ching-Yang Cheng: "Combined heat and mass transfer in natural convection flow from a vertical wavy surface in a power-law fluid saturated porous medium with thermal and mass stratification", International Communications in Heat and Mass Transfer 36, pp. 351–356, 2009
- [4] A C Cogley, W G Vincenti and S E Gilles: "Differential approximation for radiative transfer in a nongray gas near equilibrium", AIAAJ, Vol. 6, No. 3, pp. 551-556, 1968
- [5] B Devika, P V Satya Narayana and S Venkataramana: "Chemical reaction effects on MHD free convection flow in an irregular channel with porous medium", International Journal of Mathematical Archive, 4 (4), pp. 282-295, 2013
- [6] A Ebaid: "Effects of magnetic field and wall slip conditions on the peristaltic transport of a Newtonian fluid in an asymmetric channel", Phys. Letters, A Vol. 372, pp. 4493-4499, 2008
- [7] P F Fasogbon: "Convection-radiation interaction in buoyancy-induced channel flow", Global J. Pure and Appl. Math, Vol. 2, No. 2, pp. 133-146, 2006
- [8] R Grief, I S Habib and J C Lin: "Laminar convection of a radiating gas in a vertical channel", J. Fluid Mech., Vol. 46, No. 3, pp.513-520, 1971.
- [9] R Muthuraj, S Srinivas, K Nirmala: " MHD flow of a couple-stress fluid and a viscous fluid in a vertical wavy porous space with travelling thermal waves and temperature-dependent heat source", Heat Transfer – Asian Research, 43 (2), 2014
- [10] Rehana Nasrin: "Mixed magneto convection in a lid-driven cavity with a sinusoidal wavy wall and a central heat conducting body", Journal of Naval Architecture and Marine Engineering, 7, pp. 13-24, 2010
- [11] P V Satya Narayan: "Effect of variable permeability and radiation absorption on magnetohydrodynamic (MHD) mixed convective flow in a vertical wavy channel with travelling thermal waves", Propulsion and Power Research, 4 (3), pp. 150-160, 2015
- [12] S S Takhar and H Kumar: "Heat transfer with radiation in MHD free convection flow confined between a vertical wavy wall and a flat wall". Bulletin of Pure and Applied Mathematics, 1(2), pp.126-140, 2007
- [13] J C Umavathi, J Prathap Kumar and M Shekar: "Mixed convective flow of immiscible viscous fluids confined between a long vertical wavy wall and a parallel flat wall", International Journal of Engineering, Science and Technology, Vol. 2, No. 6, pp. 256-277, 2010
- [14] K Vajravelu and K S Sastri: "Free convective heat transfer in a viscous incompressible fluid confined between a long

vertical wavy wall and a parallel flat wall”, J. Fluid Mech., Vol. 86, No. 2, pp. 365-383, 1978

- [15] U N Das: “Free convective MHD flow and heat transfer in a viscous incompressible fluid confined between a long vertical wavy wall and a parallel flat wall”, Ind. J. Pure Appl. Math, Vol.23, pp. 295-304, 1992
- [16] R Taneja and N C Jain: “MHD flow with slip effects and temperature dependent heat source in a viscous incompressible fluid confined between a long vertical wavy wall and a parallel flat wall”, Def. Sci. J, Vol.54, pp.2-9, 2004

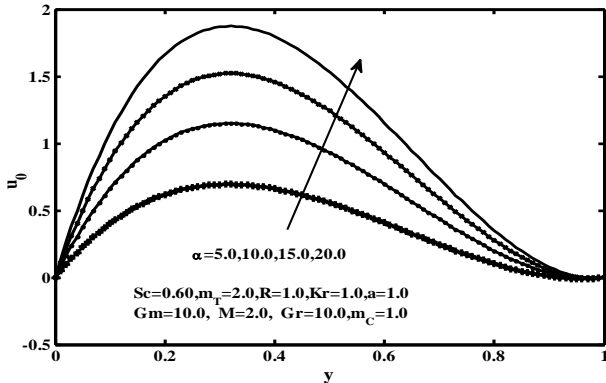


Figure (2): Zeroth-order velocity distribution for different values of  $\alpha$

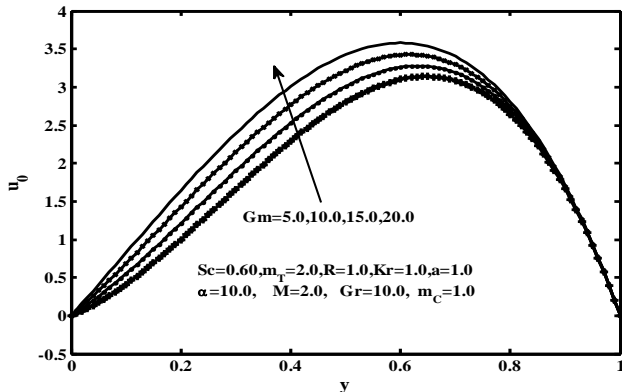


Figure (3): Zeroth-order velocity distribution for different values of  $Gm$

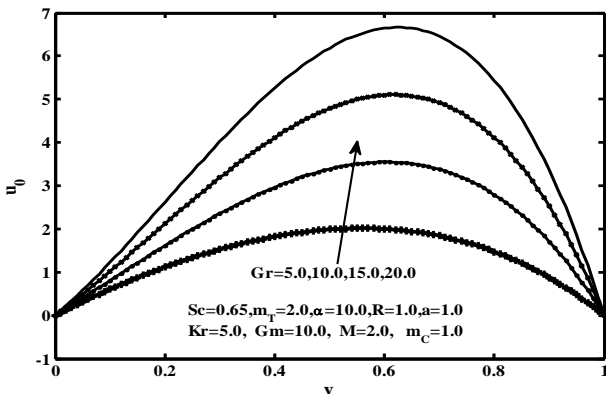


Figure (4): Zeroth-order velocity distribution for different values of  $Gr$

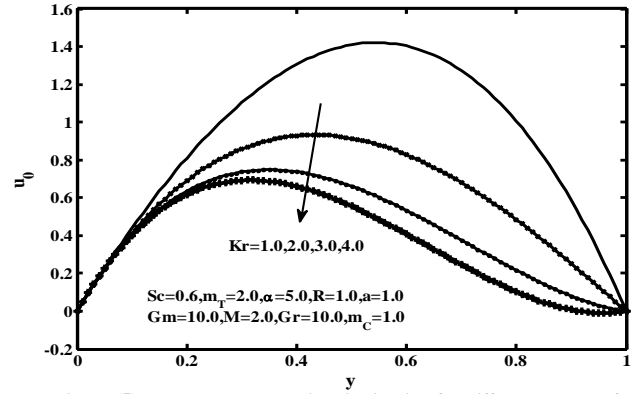


Figure (5): Zeroth-order velocity distribution for different values of  $Kr$

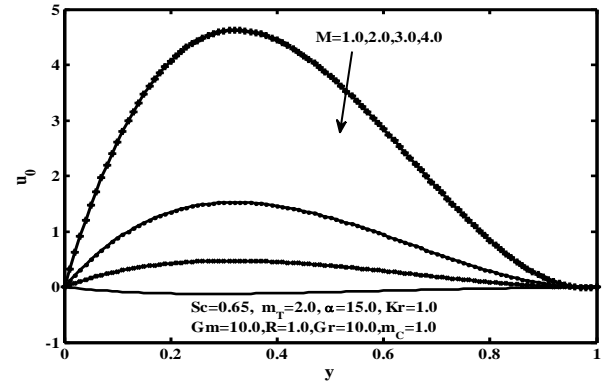


Figure (6): Zeroth-order velocity distribution for different values of  $M$

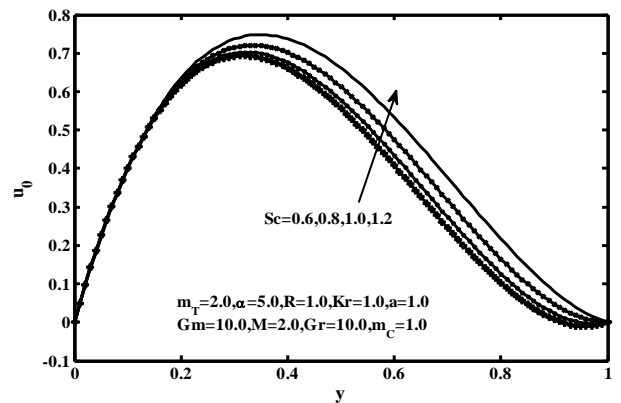


Figure (7): Zeroth-order velocity distribution for different values of  $Sc$

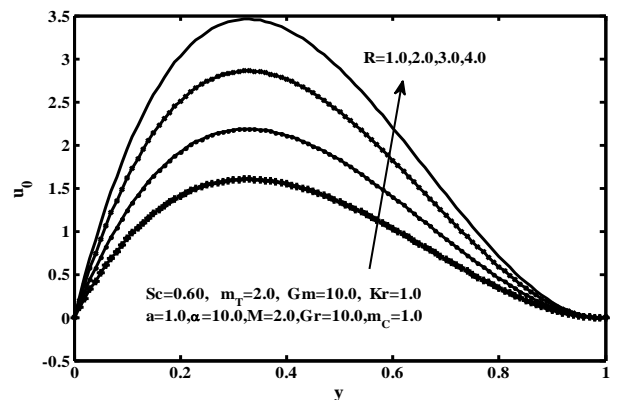


Figure (8): Zeroth-order velocity distribution for different values of  $R$

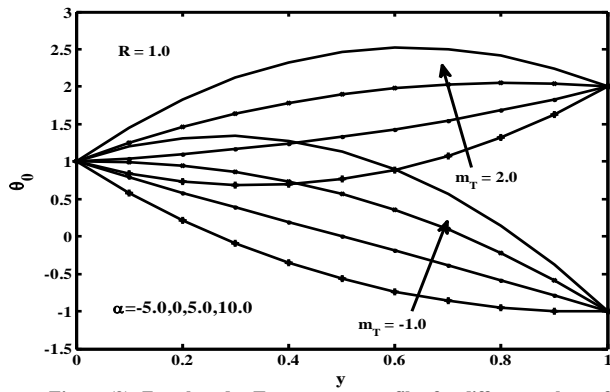
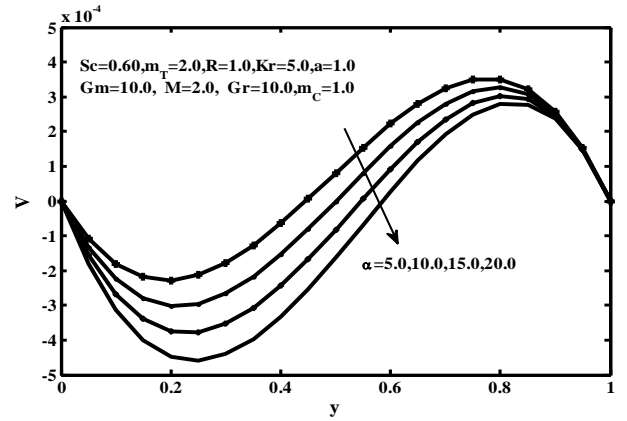


Figure (9): Zeroth-order Temperature profiles for different values of  $\alpha$



Figure(13): Cross velocity profiles for different values of  $\alpha$

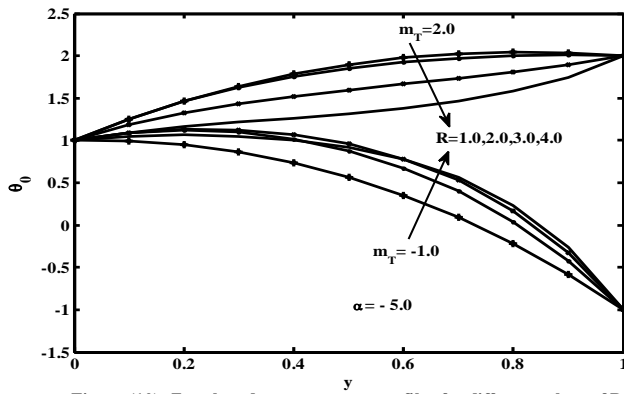
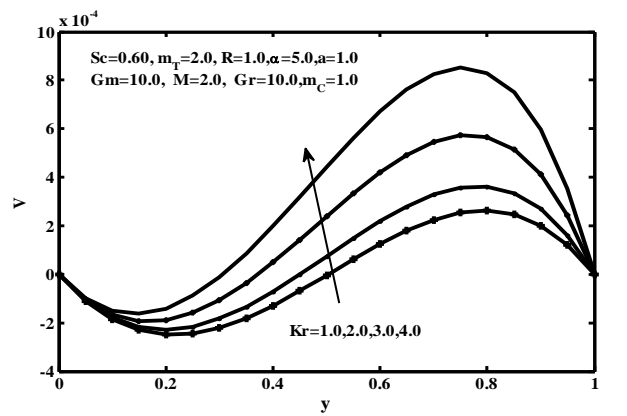


Figure (10): Zeroth-order temperature profiles for different values of  $R$



Figure(14): Cross velocity profiles for different values of  $Kr$

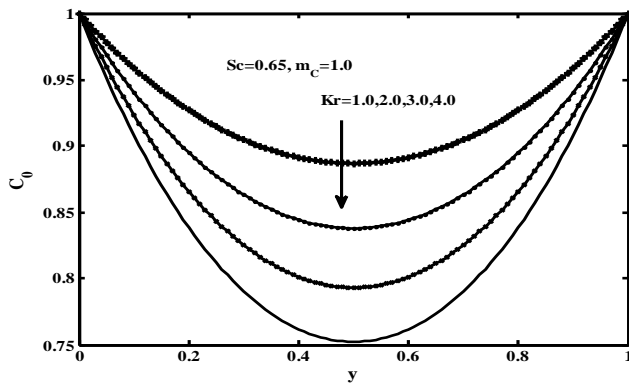


Figure (11): Concentration profiles for different values of  $Kr$

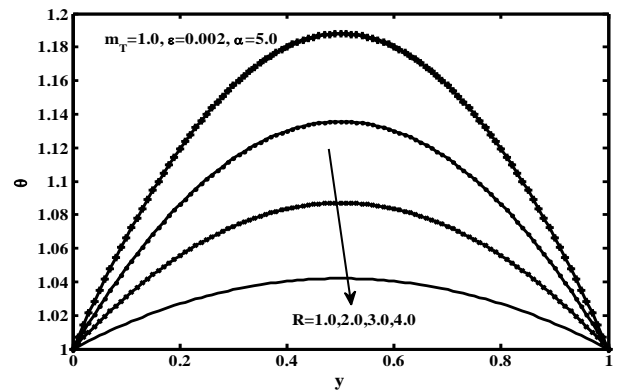


Figure (15): Temperature profiles for different values of  $R$

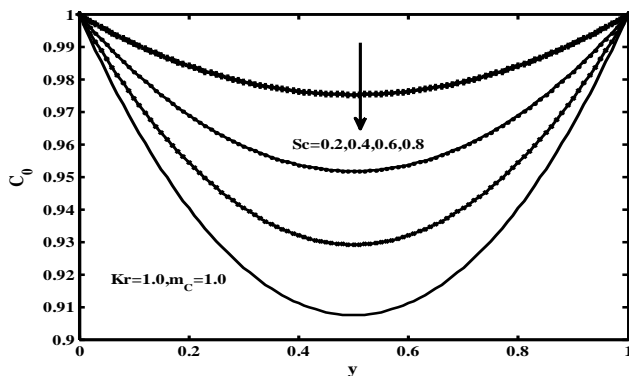


Figure (12): Concentration profiles for different values of  $Sc$

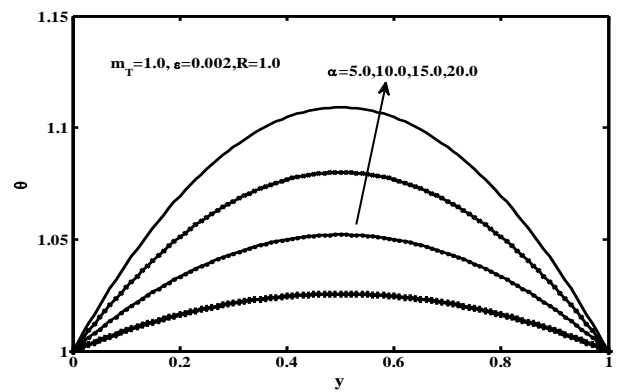


Figure (16): Temperature profiles for different values of  $\alpha$

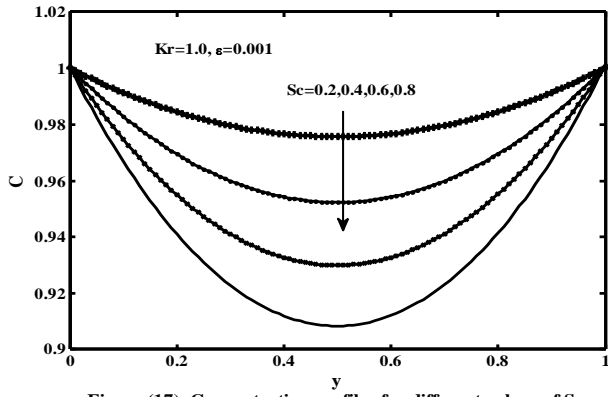


Figure (17): Concentration profiles for different values of Sc

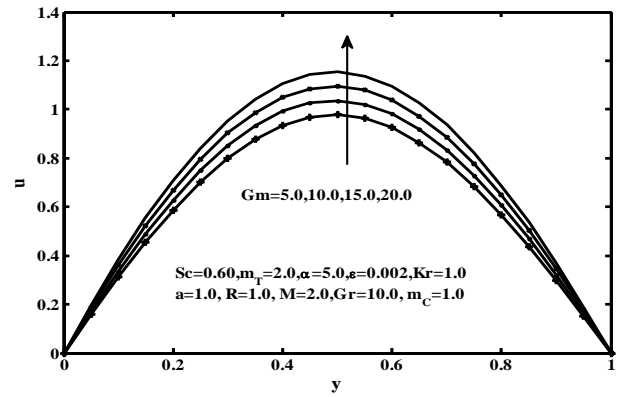


Figure (21): Velocity profiles for different values of Gm

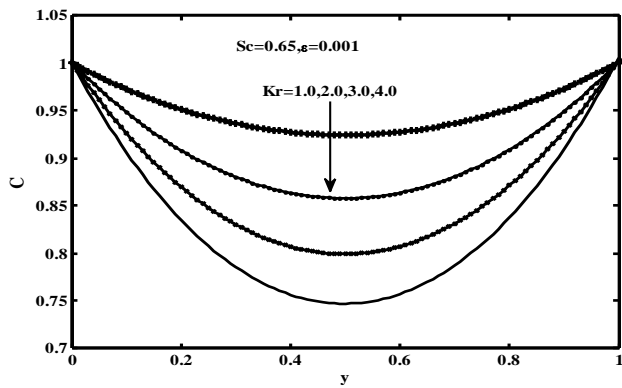


Figure (18): Concentration profiles for different values of Kr

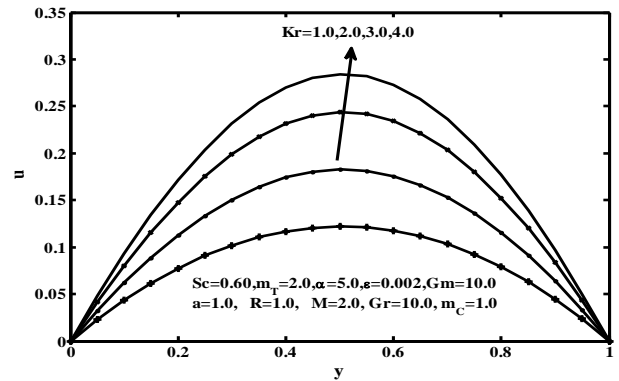


Figure (22): Velocity profiles for different values of Kr

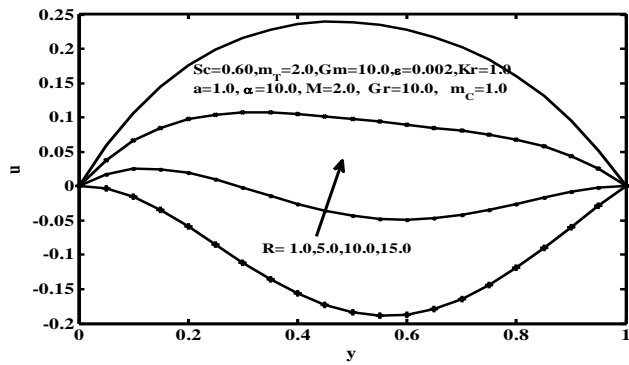


Figure (19): Velocity profiles for different values of R

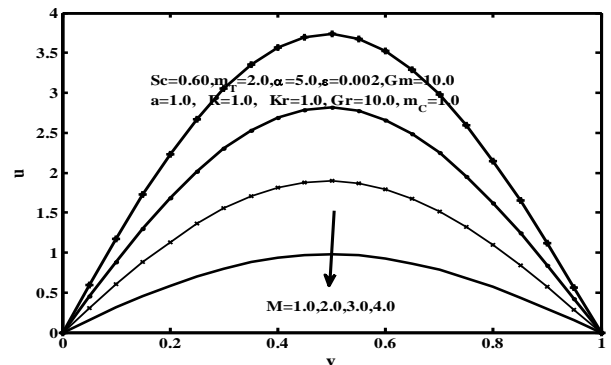


Figure (23): Velocity profiles for different values of M

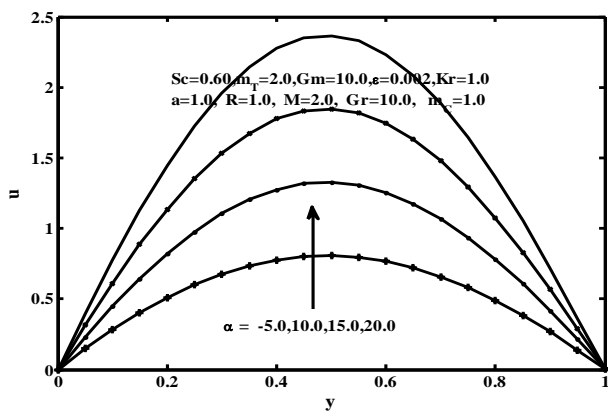


Figure (20): Velocity profiles for different values of  $\alpha$

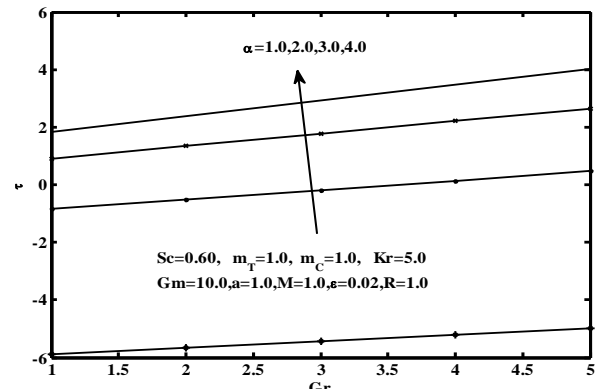


Figure (24): Skin friction for  $\alpha$  versus Gr at  $y=0$

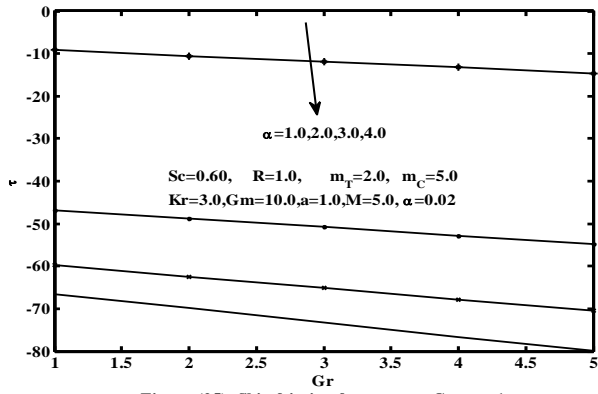


Figure (25): Skin friction for  $\alpha$  versus  $Gr$  at  $y=1$

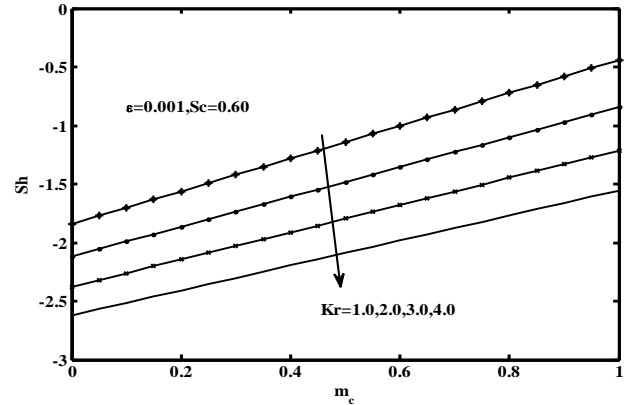


Figure (29): Sherwood number  $Kr$  versus  $m_c$  at  $y=1$

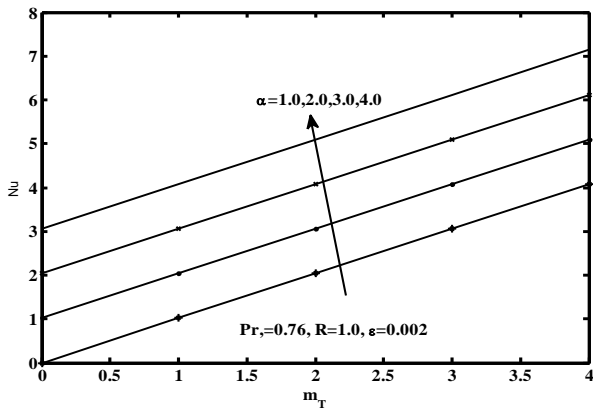


Figure (26): Nusselt number for  $\alpha$  versus  $m_T$  at  $y=0$

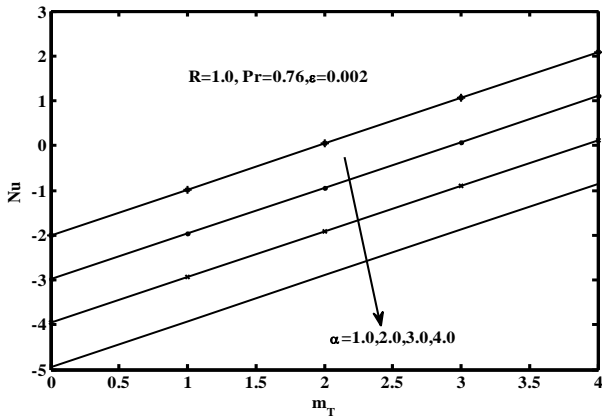


Figure (27): Nusselt number  $\alpha$  versus  $m_T$  at  $y=1$

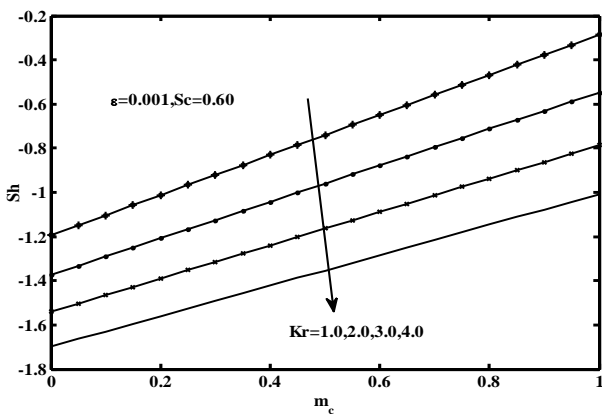


Figure (28): Sherwood number  $Kr$  versus  $m_c$  at  $y=0$